Cytogenetic Effects of Conventional and Ultra High Dose Rates of Radiation in Human Lymphocytes: Comparative Analysis in Metaphase Chromosomes and G2-PCCs

Maria B. Escalona[1], Terri L. Ryan[1], Samantha R. Gross[2], Carol J. Iddins[1] (ORCID),
Helen C. Turner[3] and Adayabalam S. Balajee[1]

[1]Cytogenetic Biodosimetry Laboratory, Radiation Emergency Assistance Center/Training Site, Oak Ridge Institute for Science and Education, Oak Ridge Associated Universities, Oak Ridge, TN, USA; [2]University of Tennessee Knoxville, Knoxville, TN, USA and [3]Center for Radiological Research, College of Physicians and Surgeons, Columbia University Irving Medical Center, New York, NY, USA

Abstract

Objectives: Ultra-high dose rate (UHDR) radiation, popularly known as FLASH, has been demonstrated to selectively kill tumor cells with minimal or negligible effects on normal cells but the biological effects induced by UHDR are not fully understood.

Methods: In this study, cytogenetic damage induced by UHDR radiation was compared with conventional dose rate (CDR) in human peripheral blood lymphocytes. Human blood samples were irradiated with 3 Gy and 8 Gy doses using 9 MeV electrons at 2 different dose rates: CDR 1 Gy/min and UHDR 600 Gy/Sec. Unstable and stable chromosomal aberrations were detected by fluorescence in situ hybridization (FISH).

Results: Reduced yields of chromosomal aberrations were observed after UHDR radiation at both radiation doses and the extent of reduction was more in colcemid arrested metaphase chromosomes than in G2-PCCs.

Conclusions: The reduced yields of chromosomal aberrations detected after UHDR of electrons may be due to rapid delivery of radiation dose within seconds, resulting in a non-uniform exposure of lymphocytes with varying levels of DNA damage induction. Future studies using well defined human equivalent in vivo and in vitro model systems are required to determine the underlying mechanisms for the FLASH effects.

CAMBRIDGE
UNIVERSITY PRESS

Ionizing radiation (IR) remains as one of the cancer treatment modalities and IR is used after surgery either alone or in combination with other chemotherapeutic agents. Conventional radiotherapy (CONV-RT) is routinely performed using photons involving 1.5 Gy - 2 Gy/ fraction over several weeks to enable the normal tissue-sparing effects of dose fractionation through faster recovery of normal tissues relative to tumor tissues. The dose fractionation strategy may pose some challenges for treating radiation-resistant brain and pancreatic cancers, and doses higher than 2 Gy can adversely affect the survival of neighboring normal cells and tissues. In recent times, FLASH radiotherapy involving ultra-high dose rate radiation (UHDR) with electrons or protons has proven effective in tumor cell killing.[1–3] Effectiveness of FLASH-RT in tumor cell killing and normal tissue sparing has been demonstrated in various animal model systems such as mice, mini pigs, and cats.[2–6] Most notably, the treatment of a 75-year-old patient afflicted with T-cell cutaneous lymphoma with FLASH-RT has paved the way for exciting new avenues for successful cancer treatment.[7]

In contrast to CONV-RT, which is delivered at the dose rate of 0.01 Gy/sec to 0.1 Gy/sec, FLASH-RT delivers radiation to the tumor site typically at a dose rate of >40 Gy/sec. Although the effectiveness of tumor control is similar for both FLASH-RT and CONV-RT, the normal tissue toxicity, unlike CONV-RT, is extremely minimal after FLASH-RT.[2,3,5,8–11] UHDR has been exploited to deliver differential effects in selective killing of tumor tissues and sparing of normal tissues but the underlying mechanisms for the FLASH effects are not clearly elucidated. Several hypotheses have been put forth for the FLASH effects based on the experimental findings on various in vivo and in vitro animal and cell model systems. Initial evidence for the involvement of hypoxia in FLASH effects came from Dewey and Boag (1959), who demonstrated an enhanced survival of bacterium *Serratia marcescens* after UHDR radiation, which was largely attributed to hypoxia.[12] This initial observation was subsequently supported by several studies on mammalian cells.[13–18] In addition to hypoxia, numerous other factors, such as radical-radical recombination,[19,20] reduced generation of reactive oxygen species,[21] depletion of nitric oxide,[22] reduced level of DNA

damage induction,[23] and differences in the metabolic rate as well as proliferation between normal and cancer cells,[21] can potentially contribute to FLASH effects.

Ionizing radiation induces a wide spectrum of DNA lesions that include single strand breaks (SSBs), double strand breaks (DSBs), base damage, and DNA-protein crosslinks either directly by excitation/ionization events or indirectly though generation of hydroxyl free radicals by hydrolysis. Among these lesions, DSBs are considered most lethal because misrepaired DNA DSBs can result in unstable and stable chromosomal aberrations and mitotic cell death depending on the severity of radiation dose. Earlier studies have provided evidence for the reduced induction of DSBs and ensuing biological endpoints after UHDR radiation.[24–27] Using antibodies specific for the 2 DSB-associated protein markers, γ-H2AX and 53BP1, reduced foci number was observed at the post irradiation time of 3 hours after FLASH radiation in normal lung fibroblasts (MRC5 and IMR-90) but not in the lung adenocarcinoma cell line (A549).[11] Also, in vivo irradiation of mice with FLASH showed reduced levels of both 53BP1 foci positive cells and 53BP1 foci number/cell in the lung cells after 3 months compared to conventional dose rate (CDR). In corroboration with the reduced number of DSBs in lung cells as evidenced by 53BP1 foci number, FLASH radiation was shown to protect the lung from radiation induced senescence in mice.[11] Reduced levels of DSBs and micronuclei in human peripheral blood lymphocytes were demonstrated after UHDR of protons[28] and electrons.[24] Using a modified Varian Clinac to generate UHDR of electrons, Garty et al.[29] documented reduced induction of dicentric chromosomes in human lymphocytes while reduced DNA damage induction in human lymphocytes was reported by UHDR radiation ex vivo as a function of dose, dose rate, and oxygen tension.[30] Cooper et al.[23] provided the evidence for UHDR-induced transient oxygen depletion in human lymphocytes that were pre-treated with and without Buthionine Sulfoximine, an antioxidant agent that inhibits glutathione synthesis.

UHDR radiation has been shown to protect the cells and tissues of various organs (lung, brain, skin, and bone marrow) in animal model systems[31] and protection is most likely to be due to reduced levels of DNA damage induction after UHDR exposure. It is known that radiation dose and dose rate can greatly affect DNA damage induction and cellular response mechanisms that involve coordinated activities of cell cycle regulation and DNA damage response (DDR) mechanisms. Further, biological effects of radiation also significantly differ between quiescent and proliferating cells.[32] Cellular survival is usually enhanced after protracted chronic low radiation dose exposures where cells have sufficient time for efficient repair of lesions that are being generated continually. However, reduced DNA damage induction coupled with enhanced cellular protection after UHDR radiation is intriguing. Understanding the biological effects of UHDR radiation is particularly relevant for the radiation biodosimetry field because delivery of a large fraction of radiation from an Improvised Nuclear Device (IND) is expected to occur at ultra-high dose rates in the initial blasts.[33] Furthermore, applicability of biodosimetry assays needs to be tested for various dose rates (low, moderate, high, and ultrahigh), particularly for UHDR in the evaluation of biodosimetry tools for radiation exposure assessment and medical triage.[33]

Here, we performed a comparative evaluation of cytogenetic effects induced by CDR and UHDR of 9 MeV electrons in human peripheral blood lymphocytes. For evaluation, both unstable (dicentrics, rings, and fragments) and stable (translocations and insertions) aberrations were analyzed in colcemid arrested metaphase chromosomes. The metaphase chromosome analysis is somewhat selective because some of the heavily damaged cells that are arrested at the G2-phase may not progress to the metaphase stage for analysis after high radiation doses (>2 Gy of acute photon-equivalent exposures). To alleviate this issue, calyculin A induced G2-PCCs were analyzed by the FISH technique[34,35] for a realistic comparison of chromosomal aberration yields after CDR and UHDR exposures. Our results indicate that the yields of chromosomal aberrations were less in the lymphocytes irradiated with UHDR compared to CDR in both metaphase chromosomes and G2-PCCs, but the extent of reduction was more in the metaphase chromosomes. In this manuscript, terms for UHDR and FLASH are interchangeably used to denote the same phenomenon.

Methods

Human Blood Collection

Whole blood samples collected from 4 donors (2 males and 2 females) were used for the current study. The entire processes of recruitment of donors, blood collection, and aliquoting of blood samples for irradiation with different doses and dose rates were carried out at the Center for Radiological Research, Columbia University Irving Medical Center (CUIMC), New York, NY. Informed consent for the blood collection was done in compliance with the protocol (AAF2671) approved by the Institutional Review Board of CUIMC. Blood samples (20 ml) were drawn by venipuncture in sodium heparinized vacutainers (BD Biosciences, Cat# 367878) and the collected blood samples were aliquoted into 1 ml Matrix™ tubes for CDR (1 Gy/min) and 0.5 ml tubes for UHDR (600 Gy/sec).

Irradiation Protocol

In this study, a decommissioned Varian Clinac irradiator was modified to deliver UHDR using 9 MeV electrons and the modifications made to the irradiator were described in an earlier study.[29] Irradiation protocol was essentially the same as described before for CDR and UHDR.[29] Each blood aliquot was irradiated with different doses (0 Gy, 3 Gy, and 8 Gy) and dose rates (CDR at 1 Gy/min) and UHDR at 600 Gy/sec using 9 MeV of electrons. Both CDR and UHDR were calculated as mean dose rates defined as $\dot{D} = n \cdot D_{pulse}/T$, where n represents the number of pulses. D_{pulse} is the mean dose per pulse determined by the source-to-surface distance (SSD) of the sample, and T represents the total irradiation time. For all the irradiations, the beam was run for 20-30 seconds using non-synchronized klystron and an electron gun to enable a fully charged pulse-forming network without delivering the beam to ensure a consistent and repeatable beam starting state for a more stable D_{pulse}. The irradiator generated a pulsed electron beam with a pulse width of 130 ns.

Delivery of CDR and UHDR

For CDR, 1 mL in matrix tubes containing the blood samples were positioned on a platform at an SSD of 171 cm. A calibrated National Institute of Standards and Technology traceable Advanced Markus ionization chamber (AMIC) was utilized to verify the delivered doses and dose rate (1 Gy/min). During irradiation, D_{pulse} experienced a drift in the range of 8-11 mGy/pulse which was compensated by adjusting the pulse repetition rate in the range of 1.5-2 Hz (one pulse "on" out of 90-120) to maintain the mean dose rate at approximately 1 Gy/min during the entire irradiation process.

Table 1. Exposure parameters for CDR and UHDR of 9 MeV electrons

CDR (1 Gy/min)			
Nominal dose rate	# of pulses	SSD (cm)	AMIC Dose (Gy)
1Gy/min	356	170	3.0
	834	170	8.0
UHDR (600 Gy/Sec)						

Nominal dose rate	# of pulses	SSD (cm)	D_{pulse} (Gy)	T (msec)	$\dot{D}$ (Gy/sec)	Film Dose (Gy)
600 Gy/s	2	25	1.5	5.6	540	2.8
	3	22	2.7	11.1	720	8.5

For the delivery of UHDR (600 Gy/sec), 4 matrix tubes with 0.5 ml of blood samples were placed in a cubic acrylic matrix tube holder. The holder was positioned on a 5-mm slab made of water-equivalent polystyrene RW3 (LAP llc, Boynton beach, FL). The 9 MeV electron beam was operated at the maximal pulse repetition rate of 180 Hz, where $T = (n-1)/(180 \text{Hz})$. The SSD of the holder was 20-30 cm. At these SSDs, the field size shrank making the depth dose shallower owing to significantly more beam divergence (see Garty et al 2022, Fig 9c). Hence, only 1 matrix tube of 0.5 ml sample was irradiated each time. The doses were delivered in 2 pulses of 1.5 Gy or 3 pulses of 2.7 Gy for 3 or 8 Gy, respectively. The target dose rate of 600 Gy/sec was a rough approximation of mean dose rate value. In practice, D_{pulse} was found to drift on different days due to internal variation in the Clinac system. The specific SSD required to deliver either 3 or 8 Gy of radiation was determined prior with a water-filled matrix tube in the holder. Because D_{pulse} for 600 Gy/sec irradiation was above 0.5 Gy/pulse, which is the Advanced Markus Ion Chamber (AMIC)'s upper limit for D_{pulse}, the AMIC was not suitable for dose monitoring in this study. Hence, the dosimetry was done using GafChromic EBT3 films. During the sample irradiations, both films and Clinac built-in ion chamber were employed to record and verify the delivered doses. Table 1 summarizes the information on the number of pulses used for 3 Gy and 8 Gy, measured doses, SSD, mean dose per pulse, irradiation duration, and mean dose rate.

Cytogenetic Analysis

Lymphocyte culture and chromosomal preparation

Mock and irradiated human blood samples were shipped from CUIMC to Oak Ridge and the aliquots of blood samples (0.5 ml) were grown for 48 hours in complete growth medium (PB-MAX, GIBCO, Carlsbad, CA, USA) at 37°C in a 5% CO_2 incubator. Colcemid (0.1 µg/ml; Karyomax, GIBCO, Carlsbad, CA, USA) was added to 1 batch of cultures for the last 24 hours and the cultures were harvested at 48 hours from the time of culture initiation. For metaphase chromosome preparation, cells were treated with a hypotonic solution (0.56% KCl) for 16–18 minutes at 37° C followed by fixation at ambient temperature in 3 changes of ice-cold acetic acid: methanol (1:3) mixture. Slides were prepared by dropping 25–30 µl of the fixed cell suspension. The slides were subsequently treated with RNase A for 30 min and processed for FISH based applications. For the preparation of G2-PCCs, calyculin A (50 nM, Enzo Lifesciences, USA) was added to the other batch of cultures for the last 30 minutes prior to harvest at

48 hours. Procedures for hypotonic treatment, fixation, and slide preparation were essentially the same as for the metaphase chromosome preparation.

Fluorescence in situ hybridization (FISH)

FISH was performed using human centromere and telomere specific Peptide Nucleic Acid (PNA, PNABio, Newbury Park, CA, USA) probes to detect unstable chromosomal aberrations in both colcemid arrested metaphase chromosomes and calyculin A-induced G2-PCCs. Unstable chromosomal aberrations (dicentrics, rings, and fragments) were analyzed in 300 cells for 3 Gy dose and 100 cells for 8 Gy dose from all the donors. Because lymphocyte proliferation is reduced at doses higher than 4 Gy, analysis was confined to 100 randomly chosen cells for 8 Gy irradiated samples. Dicentric chromosomes, ring chromosomes, and chromosome fragments were scored for unstable aberrations. Centromere and telomere staining enabled us to categorize different types of chromosome fragments: terminal with telomeric signal at 1 end, compound with telomeric signal at both ends, and interstitial with no telomeric signal. Stable chromosomal aberrations (chromosomal exchange events involving insertions, balanced and unbalanced translocations) were analyzed using a cocktail of DNA probes specific for chromosomes 1 (red), 2 (yellow), and 4 (green) procured from MetaSystems, Boston, MA, USA. Hybridizations were carried out separately for centromere/telomere and chromosome specific painting probes for detecting the unstable and stable chromosomal aberrations. In the current study, all the chromosomal exchange events were scored as color junctions between painted as well as between painted and non-painted chromosomes. The procedures used for FISH using centromere/telomere probes and chromosome specific paints were essentially the same as described in our earlier publications.[34,36–38] After the hybridization and post-hybridization washings, slides were stained with DAPI (4',6-diamidino-2-phenylindole; Vector Laboratories, Burlingame, CA, USA). Images were initially captured using the metaphase finder algorithm (MetaSystems) at 10X objective lens and later at 63X objective lens using an epifluorescence microscope (Carl Zeiss). Images of metaphase chromosomes and G2-PCCs captured at 63X objective lens were analyzed using the ISIS software (MetaSystems, Boston, MA, USA).

Statistical Analysis

The yields of unstable and stable chromosomal aberrations obtained after CDR and UHDR exposures of electrons were expressed as mean ± standard error of the mean (SEM). Values of the dispersion index and U test were calculated using a commercially available BioDose algorithm. Student's t test was performed and a P value of less than 0.05 was considered significant.

Results

Effects of CDR and UHDR on Unstable Chromosomal Aberrations in Metaphase Chromosomes and G2-PCCs

In this study, unstable and stable chromosomal aberrations were analyzed as a function of dose and dose rate in colcemid-arrested metaphase chromosomes and calyculin A-induced G2-PCCs of human lymphocytes. A radiation dose-dependent increase in unstable aberrations was observed in both metaphase chromosomes and G2-PCCs after 3 Gy and 8 Gy of electrons but the aberration yields were differentially reduced in the metaphase

chromosomes and G2-PCCs as a function of dose rate (1 Gy/min vs 600 Gy/sec) at both radiation doses. Representative pictures of centromere and telomere FISH-stained metaphase chromosomes and G2-PCCs are shown in Figure 1. Data obtained on the yields of dicentric chromosomes in the metaphase chromosomes and in the G2-PCCs from the samples of 2 donors are shown in Tables 2 and 3. The dicentric chromosome yields in the blood samples irradiated with UHDR at different electrons doses (3 Gy and 8 Gy) were reduced by 19-27% for 3 Gy and 46-48% for 8 Gy in the metaphase cells of both donors relative to samples irradiated with CDR (the dicentric chromosome yields observed in lymphocytes irradiated with 3 Gy and 8 Gy at CDR were considered as 100%). It is worth noting that the percentages of cells detected without dicentrics were higher after UHDR exposure of 3 Gy (66.66% for donor 1; 61.33% for donor 2) and 8 Gy (35% for donor 1; 27% for donor 2) relative to CDR exposure of 3 Gy (52.66% for donor 1; 54% for donor 2) and 8 Gy (5% for donor 1; 2% for donor 2) in the metaphase chromosomes. As a result, values of the dispersion index (2.23 for donor 1; 2.07 for donor 2) and U test were higher (8.69 for donor 1; 7.54 for donor 2), indicating the over-dispersion pattern of dicentric chromosome distribution (Table 2) after 8 Gy of UHDR in the metaphase chromosomes. In striking contrast to metaphase chromosomes, dicentric yields were only marginally reduced by 5%-15% in calyculin-induced G2-PCCs at both doses (3 Gy and 8 Gy) and dose rates (1 Gy/min and 600 Gy/sec; Table 3) in the samples of the 2 donors. The reduction seen in the dicentric

chromosome yields of G2-PCCs after UHDR was not statistically significant. Only 1 sample of donor 1 irradiated with 8 Gy at UHDR showed overdispersion of dicentric chromosome distribution in the G2-PCCs with the U test value of 2.36 (Table 3). Frequencies for all the unstable aberrations (dicentric chromosomes, rings, and fragments) detected in the metaphase chromosomes and G2-PCCs of both donor samples at both radiation doses and dose rates are summarized in Tables 4 and 5. All the 3 types of chromosomal fragments were included in the analysis (terminal fragments with telomeric signals at 1 end, interstitial fragments lacking the telomeric signal, and compound fragments with telomeric signals at both ends, resulting from the fusion of terminal fragments typically from 2 broken chromosomes; Figure 1). The frequencies for terminal, interstitial, and compound fragments were pooled together for both metaphase chromosomes (Table 4) and G2-PCCs (Table 5). Calyculin A-induced G2-PCCs prepared from sham irradiated cells (0 Gy) showed increased numbers of fragments in both donors compared to metaphase chromosomes (Tables 4 and 5). The compound fragments with telomeric signals at both ends were formed predominantly (more than 50% of the total fragments), followed by terminal and interstitial fragments, after exposure to both radiation doses and dose rates in the metaphase chromosomes and G2-PCCs. The reduced yields of all the unstable aberrations observed after UHDR in the samples of both donors (Figure 2) were found to be statistically significant only for the metaphase chromosomes (*t* test *P* value was less than 0.05 for both
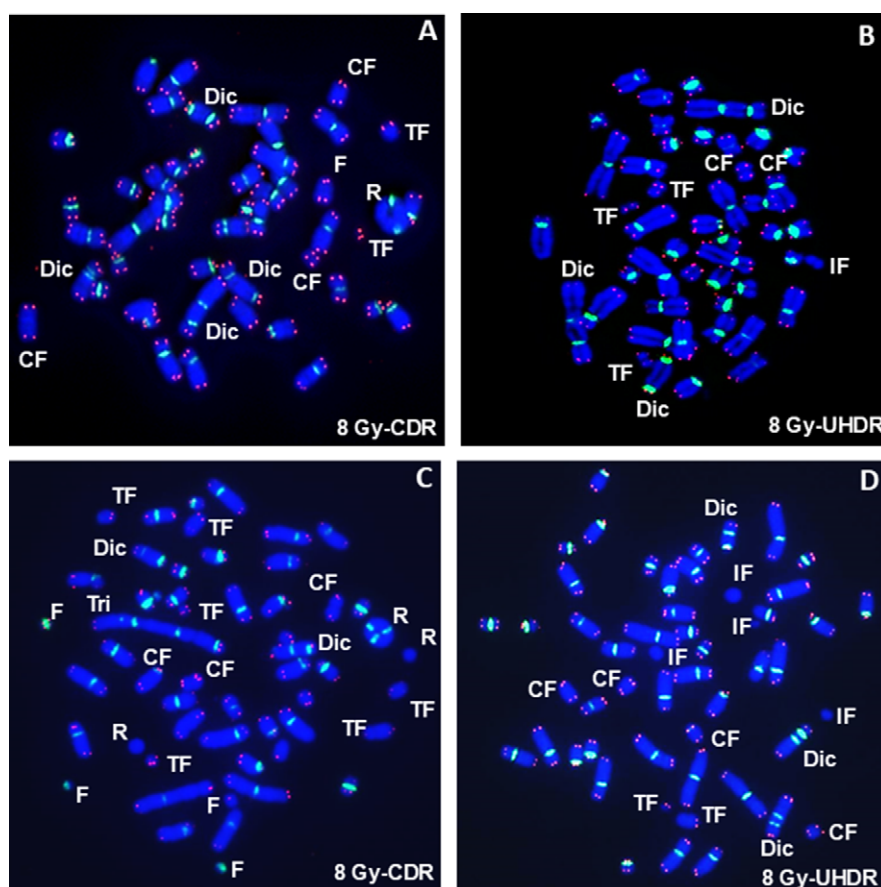

Figure 1. Representative pictures of metaphase chromosomes (A and B) and G2-PCCs (C and D) after 8 Gy of electrons at 2 different dose rates (CDR-1 Gy/min and UHDR- 600 Gy/sec). Calyculin A-induced G2-PCCs and colcemid-arrested metaphase chromosomes were hybridized to human pan centromeric (green color) and telomeric (red color) PNA (Peptide Nucleic Acid) probes. Aberrant chromosomes are marked: Dic-dicentric, Tri-tricentric, R-ring, IF-interstitial fragment, TF-terminal fragment, and CF-compound fragment. Note the presence of dicentric and tricentric ring chromosomes after 8 Gy of electrons delivered at 1 Gy/min.

Table 2. Analysis of dicentric chromosomes induced by CDR and UHDR of electrons in metaphase chromosomes

Sample	Dose and dose rate	Cells	Dicentrics	Distribution of Dicentrics											Mean ± SE	Di	U
				0	1	2	3	4	5	6	7	8	9	10			
Donor 1	0 Gy (1 Gy/Min)	300	2	298	2	0	0	0	0	0	0	0	0	0	0.01 ± 0	1.00	−0.06
	0Gy (600 Gy/sec)	300	0	0	0	0	0	0	0	0	0	0	0	0	0	0	0
	3 Gy (1 Gy/min)	300	198	158	96	37	8	1	0	0	0	0	0	0	0.66 ± 0.05	1.02	0.25
	3 Gy (600 Gy/sec)	300	143	185	91	20	4	0	0	0	0	0	0	0	0.48 ± 0.04	0.97	−0.32
	8 Gy (1Gy/min)	100	376	5	10	10	26	13	13	14	6	2	1	0	3.76 ± 0.20	1.10	0.72
	8 Gy (600 Gy/sec)	100	193	35	22	6	16	6	6	6	3	0	0	0	1.93 ± 0.21	2.23	8.69*
Donor 2	0 Gy (1 Gy/min)	300	0	0	0	0	0	0	0	0	0	0	0	0	0	0	0
	0 Gy (600 Gy/sec)	300	0	0	0	0	0	0	0	0	0	0	0	0	0	0	0
	3 Gy (1 Gy/min)	300	186	162	98	32	8	0	0	0	0	0	0	0	0.62 ± 0.05	0.99	−0.18
	3 Gy (600 Gy/sec)	300	149	184	87	25	4	0	0	0	0	0	0	0	0.50 ± 0.04	1.00	0.04
	8 Gy (1 Gy/min)	100	393	2	10	12	18	22	15	9	9	2	1	0	3.93 ± 0.20	0.97	−0.23
	8 Gy (600 Gy/sec)	100	209	27	23	16	12	8	5	3	5	1	0	0	2.09 ± 0.21	2.07	7.54*

Di- Dispersion index; U test value higher than 1.96 indicates over dispersion (*).

Table 3. Analysis of dicentric chromosomes induced by CDR and UHDR of electrons in calyculin A-induced G2-PCCs

Sample	Dose and dose rate	Cells	Dicentrics	Distribution of dicentrics												Mean ± SE	Di	U
				0	1	2	3	4	5	6	7	8	9	10	11			
Donor 1 (Male)	0 Gy (1 Gy/min)	300	0	300	0	0	0	0	0	0	0	0	0	0	0	0.01 ± 0	1.00	−0.06
	0 Gy (600 Gy/sec)	300	2	298	2	0	0	0	0	0	0	0	0	0	0	0	0	0
	3 Gy (1 Gy/min)	300	256	114	128	46	12	0	0	0	0	0	0	0	0	0.85 ± 0.05	0.79	−2.57
	3 Gy (600 Gy/sec)	300	238	133	113	41	10	2	1	0	0	0	0	0	0	0.79 ± 0.05	0.99	−0.10
	8 Gy (1Gy/min)	100	430	0	4	8	21	26	21	10	5	4	0	0	1	4.30 ± 0.17	0.70	−2.10
	8 Gy (600 Gy/sec)	100	380	6	8	15	20	18	12	9	5	4	2	0	1	3.80 ± 0.22	1.33	2.32*
Donor 2 (Female)	0 Gy (1 Gy/min)	300	0	300	0	0	0	0	0	0	0	0	0	0	0	0	0	0
	0 Gy (600 Gy/sec)	300	0	300	0	0	0	0	0	0	0	0	0	0	0	0	0	0
	3 Gy (1 Gy/min)	300	222	142	107	40	9	2	0	0	0	0	0	0	0	0.74 ± 0.05	0.98	−0.31
	3 Gy (600 Gy/sec)	300	185	156	108	32	3	1	0	0	0	0	0	0	0	0.62 ± 0.04	0.89	−1.29
	8 Gy (1 Gy/min)	100	349	2	10	17	28	17	14	4	6	1	1	0	0	3.49 ± 0.18	0.92	−0.58
	8 Gy (600 Gy/sec)	100	335	5	9	20	18	25	10	9	4	0	0	0	0	3.35 ± 0.17	0.90	−0.70

Di-Dispersion index; U test value higher than 1.96 indicates over dispersion (*).

3 Gy ($P = 0.004$) and 8 Gy ($P = 0.04$) but not for the G2-PCCs. In general, frequencies of total unstable aberrations induced per cell were 1.3-2.2 folds higher in the G2-PCCs than in the metaphase chromosomes, except for 1 sample from donor 2 (aberration frequency/cell for 8 Gy: CDR 10.44 ± 1.10 for metaphase chromosomes and 10.68 ±1.11 for G2-PCCs). Interestingly, differences in the induction of multicentric chromosomes (abnormal chromosomes with 3 or more centromeres resulting from the mis-rejoining of 3 or more broken chromosomes with intact centromeres) were observed in the samples of both donors between CDR and UHDR exposures at 8 Gy. Pooled values of multicentric chromosomes in the samples of both donors are shown in Figure 3. After exposure to 8 Gy of electrons at UHDR, the yields of multicentric chromosomes were reduced by 54.85% in the metaphase chromosomes and by 39.29% in the G2-PCCs relative to CDR-treated samples. The

reduced yields of multicentric chromosomes (3 or >3 centromeres) observed were found to be statistically significant ($P=0.04$) after UHDR of 8 Gy in both metaphase chromosomes and G2-PCCs.

Effects of CDR and UHDR of Electrons on Stable Chromosomal Aberrations

Blood samples from 2 donors (1 male [donor 3] and 1 female [donor 4]) were used to determine the effects of dose (3 Gy and 8 Gy) and dose rate (1 Gy/min and 600 Gy/sec) on stable chromosomal aberrations (translocations and insertions). Representative pictures of metaphase chromosomes and G2-PCCs hybridized with a cocktail of DNA probes specific for chromosomes 1, 2, and 4 are shown in Figure 4. Color junctions reflective of chromosome exchanges were scored to avoid the complexities in classifying

Table 4. Unstable chromosome aberrations induced by CDR and UHDR of electrons in metaphase chromosomes

Sample	Dose and dose rate	Cells scored	Dicentrics	Rings	Fragments	Total aberrations	Yield ± SE
Donor 1 (Male)	0 Gy (1 Gy/min)	300	2	0	2	4	0.01 ± 0.006
	0 Gy (600 Gy/sec)	300	0	0	3	3	0.01 ± 0.005
	3 Gy (1 Gy/min)	300	198	20	300	518	1.72 ± 0.12
	3 Gy (600 Gy/sec)	300	143	17	248	408	1.36 ± 0.10
	8 Gy (1 Gy/min)	100	376	31	476	883	8.83 ± 0.93
	8 Gy (600 Gy/sec)	100	193	20	301	514	5.14 ± 0.56
Donor 2 (Female)	0 Gy (1 Gy/min)	300	0	0	4	4	0.01 ± 0.006
	0 Gy (600 Gy/sec)	300	0	0	5	5	0.01 ± 0.007
	3 Gy (1 Gy/min)	300	186	19	304	509	1.69 ± 0.12
	3 Gy (600 Gy/sec)	300	149	19	228	396	1.32 ± 0.10
	8 Gy (1 Gy/min)	100	393	36	615	1044	10.44 ± 1.10
	8 Gy (600 Gy/sec)	100	209	23	351	583	5.83 ± 0.63

Table 5. Unstable chromosome aberrations induced by CDR and UHDR of electrons in G2-PCCs

Sample	Dose and dose rate	Cells scored	Dicentrics	Rings	Fragments	Total aberrations	Yield ± SE
Donor 1 (Male)	0 Gy (1 Gy/min)	300	0	0	23	23	0.07 ± 0.01
	0 Gy (600 Gy/sec)	300	2	1	86	89	0.29 ± 0.03
	3 Gy (1 Gy/min)	300	256	24	532	812	2.70 ± 0.18
	3 Gy (600 Gy/sec)	300	238	44	461	743	2.47 ± 0.17
	8 Gy (1 Gy/min)	100	430	80	801	1311	13.11 ± 1.36
	8 Gy (600 Gy/sec)	100	380	59	703	1142	11.42 ± 1.20
Donor 2 (Female)	0 Gy (1 Gy/min)	300	0	0	28	28	0.09 ± 0.01
	0 Gy (600 Gy/sec)	300	0	0	34	34	0.11 ± 0.02
	3 Gy (1 Gy/min)	300	222	47	418	687	2.29 ± 0.16
	3 Gy (600 Gy/sec)	300	185	39	378	602	2.00 ± 0.14
	8 Gy (1 Gy/min)	100	349	64	655	1068	10.68 ± 1.11
	8 Gy (600 Gy/sec)	100	335	55	620	1010	10.10 ± 1.06

simple and complex (involving 2 or more chromosomes) exchanges. All the exchange type aberrations involving painted (1, 2, and 4) and non-painted chromosomes (rest of the non-painted chromosomes) were analyzed. Data on color junctions detected after 3 Gy and 8 Gy of electrons at CDR and UHDR in the metaphase chromosomes of donor 3 and donor 4 samples are shown together with values for dispersion index (Di) and U test in Table 6 and Figure 5. The U test values for both CDR and UHDR for the samples of donors 3 and 4 were higher than 1.96, indicating the over dispersion of chromosomal exchange events in the metaphase chromosomes. As with dicentrics, the frequency of color junctions detected per cell for UHDR showed a reduction by 28.52% for 3 Gy and 23.72% for 8 Gy in donor 3 and 38.85% for 3 Gy and 23.72% for 8 Gy in donor 4 compared to CDR (frequencies of color junctions observed in CDR-treated samples were considered as 100%). The dispersion index was higher than 1.96 for all the samples and the U test values ranged from 7.97-20.35, indicating the over dispersion pattern of color junctions in the metaphase chromosomes. The frequencies of color junctions detected in the G2-PCCs of both

donors after CDR and UHDR of electrons are shown in Table 7 and Figure 5. Like metaphase chromosomes, the value of dispersion index was higher than 1 for all the samples and the U test values ranged from 3.31-14.09, indicating the over dispersion of color junctions for both CDR and UHDR exposures in the G2-PCCs.

Discussion

FLASH-RT delivered at ultrahigh dose rates (>40 Gy/Sec) is steadily emerging as an effective therapeutic tool for cancer. A distinct advantage of FLASH-RT is the sparing of normal tissues from radiation injuries, thereby minimizing adverse side effects. The mechanistic basis for the differential effects of FLASH-RT on normal and tumor tissues is not clearly understood. Understanding the DNA damage response mechanisms (DDR) for FLASH radiation is critical for gaining insights into how cells respond to UHDR radiation and to determine whether UHDR-induced DNA damage repair mechanisms differ from those for CDR. In this study, effects of radiation dose and dose rate on chromosomal aberrations were
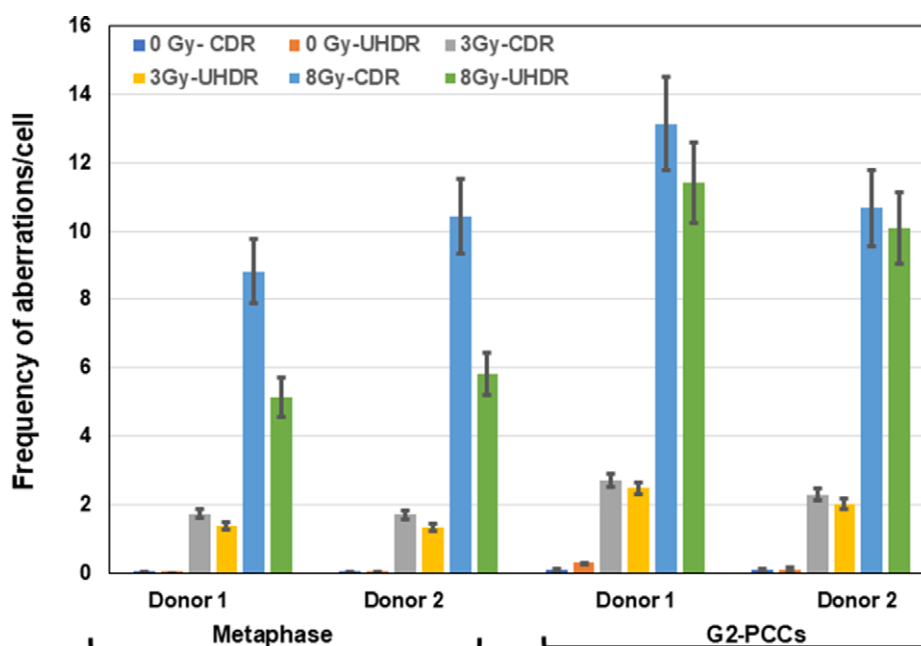
Figure 2. Analysis of unstable chromosomal aberrations induced by CDR (1 Gy/min) and UHDR (600 Gy/sec) of electrons in metaphase chromosomes and calyculin A-induced G2-PCCs at different doses (3 Gy and 8 Gy). Pooled values of the donors for all the unstable chromosomal aberrations (dicentrics, rings, and fragments) are shown for the 2 donors. Error bars indicate SEM.
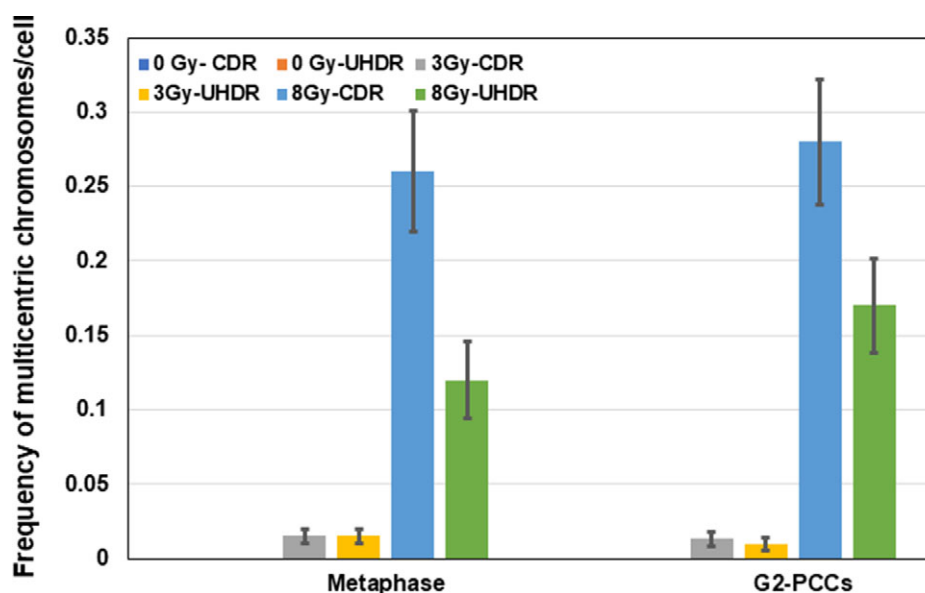

Figure 3. Induction of multicentric chromosomes (chromosomes with 3 or more centromeres) after CDR and UHDR exposure of human lymphocytes to electrons. Pooled average values for the multicentric chromosomes (chromosomes with 3 or more centromeres) are shown. Error bars indicate SEM.

evaluated in metaphase chromosomes and calyculin A-induced G2-PCCs by analyzing different types of unstable and stable chromosomal aberrations.

Our study shows that the yields of unstable chromosomal aberrations (dicentrics, rings, and fragments) were reduced after UHDR exposure relative to CDR exposure, but the reduction was higher at a dose of 8 Gy than at a dose of 3 Gy in the metaphase chromosomes of both donors (an average of an approximately 20% reduction for 3 Gy and 42% reduction for 8 Gy). In contrast to metaphase chromosomes, only a modest decline (10.70% for 3 Gy and 9.05% for 8 Gy) in unstable chromosomal aberrations was observed in the G2-PCCs

after UHDR without any dose dependency. Nevertheless, a significant effect was observed for the frequencies of multicentric chromosomes that showed a reduction after 8 Gy of UHDR in both metaphase chromosomes (0.26 ± 0.04/cell for CDR and 0.12 ± 0.02/cell for UHDR) and G2-PCCs (0.28 ± 0.04 for CDR and 0.17 ± 0.03 for UHDR), albeit with a higher reduction in the metaphase chromosomes. Like unstable chromosomal aberrations, stable chromosomal aberrations (translocations and insertions) were reduced after UHDR at both radiation doses in both metaphase chromosomes (33.65% reduction for 3 Gy and 24.22% reduction for 8 Gy relative to 100% of CDR) and G2-PCCs (25.87% reduction
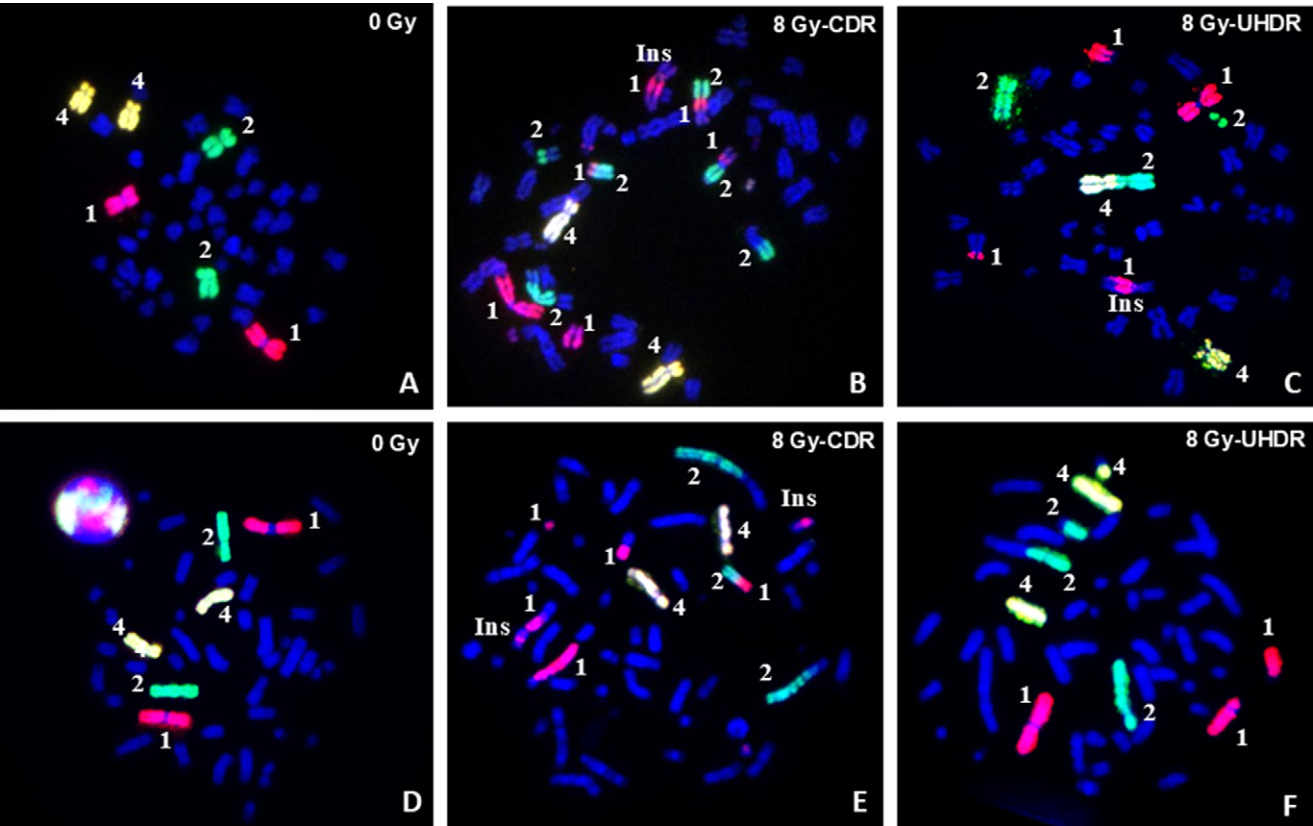
Figure 4. Representative pictures of metaphase chromosomes (A, B, and C) and G2-PCCs (D, E, and F) after 8 Gy exposure of electrons at 2 different dose rates (CDR-1 Gy/min and UHDR- 600 Gy/sec). Colcemid-arrested metaphase chromosomes and calyculin A-induced G2-PCCs were hybridized to a cocktail of DNA probes specific for chromosomes 1 (Red), 2 (Green), and 4 (Yellow). Chromosome exchange events between painted (1, 2, and 4) as well as between painted and non-painted (DAPI stained chromosomes in blue color) chromosomes are shown. Ins-Insertions.

Table 6. Analysis of color junctions induced by CDR and UHDR of 9MeV electrons in metaphase chromosomes

Sample	Dose and dose rate	Cells scored	No. color junctions	Mean ±SE	DI	U
Donor 3 (Male)	0 Gy	300	0	0	0	0
	3 Gy (1 Gy/min)	300	189	0.63 ± 0.07	2.47	18.06
	3 Gy (600 Gy/sec)	300	134	0.45 ± 0.06	2.08	13.29
	8 Gy (1 Gy/min)	100	371	3.71 ± 0.30	2.36	9.62
	8 Gy (600 Gy/sec)	100	283	2.83 ± 0.27	2.58	11.17
Donor 4 (Female)	0 Gy	300	0	0	0	0
	3 Gy (1 Gy/min)	300	290	0.97 ± 0.08	2.08	13.25
	3 Gy (600 Gy/sec)	300	181	0.60 ± 0.07	2.66	20.35
	8 Gy (1 Gy/min)	100	468	4.68 ± 0.32	2.13	7.97
	8 Gy (600 Gy/sec)	100	357	3.57 ± 0.30	2.50	10.59

for 3 Gy and 12.40% reduction for 8 Gy) without any dose dependency. In sharp contrast to our observations, Barghouth et al.[39] demonstrated that the translocations measured by high throughput rejoin and genome wide translocation using yeast Cas9 "bait" in the HEK293 cells were essentially the same after CDR and UHDR. These contradictory results may be due to differences in the techniques and cell systems used. Our study utilized primary non-transformed human peripheral blood lymphocytes, but Barghouth et al.[40] utilized immortalized human embryonic kidney cell line HEK293. In our study, exchanges in the range of 1-5 Mb were analyzed using the cocktail of chromosome painting probes, while translocations at the sites of bait proximal repair were analyzed at the single nucleotide resolution by Barghouth et al.[39] Currently, it is not clear whether the radio responses to UHDR at acute high radiation doses will be different for replicatively quiescent primary lymphocytes and exponentially growing immortalized cells. Future studies
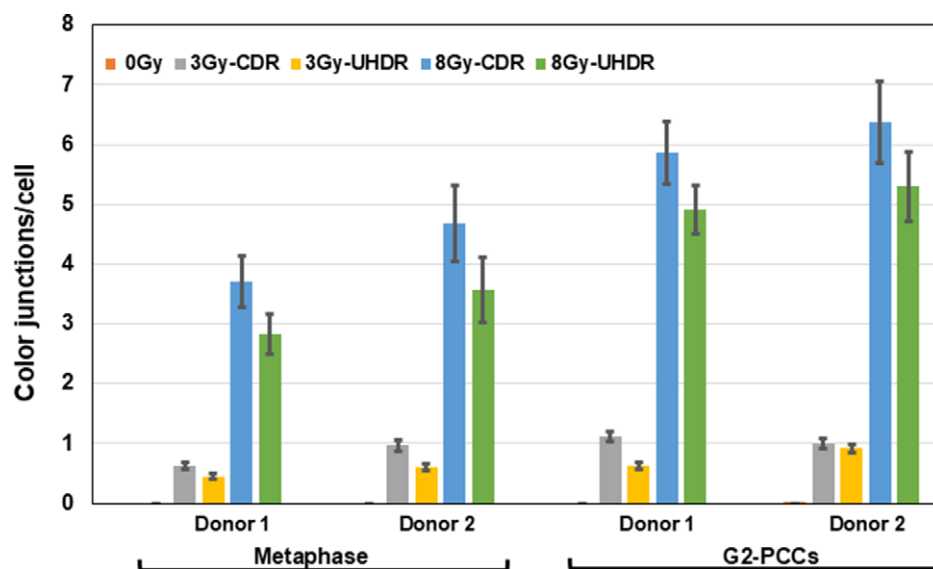
Figure 5. Analysis of stable chromosomal aberrations in human lymphocytes after exposure to CDR and UHDR of electrons. Chromosomal exchange events (translocations and insertions) were scored as color junctions in the samples of donors 3 and 4. The frequencies of color junctions/cell are shown for the metaphase chromosomes and G2-PCCs. Color junctions are inclusive of exchanges between painted as well as painted and non-painted chromosomes. Error bars indicate SEM.

Table 7. Analysis of color junctions induced by CDR and UHDR of 9MeV electrons in G2-PCCs

Sample	Dose and dose rate	Cells scored	No. color junctions	Mean ± SE	DI	U
Donor 3 (Male)	0 Gy	300	0	0	0	0
	3 Gy (1 Gy/min)	300	337	1.12 ± 0.09	2.15	14.09
	3 Gy (600 Gy/sec)	300	190	0.63 ± 0.07	2.43	17.50
	8 Gy (1 Gy/min)	100	586	5.86 ± 0.32	1.80	5.61
	8 Gy (600 Gy/sec)	100	491	4.91 ± 0.35	2.43	10.09
Donor 4 (Female)	0 Gy	300	3	0.01 ± 0.01	1.66	9.92
	3 Gy (1 Gy/min)	300	299	1.00 ± 0.08	1.88	10.73
	3 Gy (600 Gy/sec)	300	275	0.92 ± 0.08	2.11	13.62
	8 Gy (1 Gy/min)	100	637	6.37 ± 0.31	1.47	3.31
	8 Gy (600 Gy/sec)	100	530	5.30 ± 0.38	2.72	12.08

are required to verify whether the effects of UHDR on DNA damage induction/repair mechanisms would be different for proliferating and non-proliferating cells.

Our results suggest two possibilities for the reduced yields of chromosomal aberrations after UHDR: (I) DNA damage is inflicted in a non-uniform manner due to rapid delivery of radiation dose within seconds and (II) Heterogeneous DNA damage induction among the cells that are targeted by UHDR. In agreement with the first possibility, it has been proposed that FLASH-RT at the dose rate of 40 Gy/sec or more is likely to damage a smaller fraction of lymphocytes, thereby preserving the immune response by reducing radiation-induced lymphopenia in contrast to CONV-RT.[41] Although this possibility seems more relevant for the FLASH-RT in vivo, observations of increased percentages of cells without any detectable aberrations specifically after UHDR exposure in the metaphase cells suggest a non-uniform exposure of lymphocytes due to a rapid delivery of dose within seconds. Like metaphase chromosomes, the number of cells without chromosomal aberrations also increased in the G2-PCCs after UHDR.

The second possibility of heterogeneous DNA damage induction by UHDR is supported by the overdispersion pattern of dicentric chromosomes detected after 8 Gy in the metaphase chromosomes. Our results are in corroboration with the demonstration of a reduced level of dicentric chromosomes[29] and γ-h2AX foci formation[28] after UHDR radiation with electrons and protons in human lymphocytes and fibroblasts. Furthermore, irradiation with multiple pulses between 10-50 ms intervals was demonstrated to result in reduced DNA damage accompanied by enhanced cell survival.[42] The formation of multicentric chromosomes (abnormal chromosomes with more than 2 centromeres due to mis-rejoining of 3 or more broken chromosomes with intact centromeres) occurs more frequently at radiation doses higher than 2 Gy. Although no attempt was made in this study to quantify the distribution of DSBs in individual cells, the significantly reduced yields of multicentric chromosomes (but not their lack of induction) in the metaphase chromosomes and G2-PCCs after UHDR of electrons suggest a likely possibility that UHDR radiation-induced DNA damage is heterogeneous among the targeted cells with some cells having

more DNA damage than others due to a rapid delivery of radiation dose within seconds. This notion is supported by the differences observed in the distribution pattern of dicentric chromosomes in the damaged cells (cells with 1 dicentric, 2 dicentrics, and so on) for the metaphases (Table 2) and the G2-PCCs (Table 3), owing to varying levels of DNA damage, particularly DSBs. In corroboration with our study, delivery of radiation dose of 20 Gy at UHDR was shown to induce less DSBs and dicentric chromosomes relative to CDR in earlier studies performed several decades ago.[26,27] It was recently demonstrated that the DNA strand breaks and clustered DNA damage were reduced by 1.3-3.5 folds in the plasmid DNA after UHDR at 55 and 125 Gy/sec[43] and the reduced DNA damage induction was found to be independent of hydroxyl radical scavenging and oxygen depletion. In the lack of micro dosimetry analysis at the individual cellular level, it is difficult to assess whether a combination of non-uniform exposure and heterogeneous DNA damage induction among the targeted cells contributes to reduced chromosomal aberrations after UHDR exposure.

In the current study, both unstable and stable chromosomal aberrations showed a higher reduction in the metaphase chromosomes than in the G2-PCCs. It is well known that radiation induced DNA damage causes cell cycle arrest, and the damaged cells accumulate at the G2-M phase as a function of radiation dose.[44] The marked reduction in chromosomal aberrations observed in the metaphase cells may be probably due to the arrest of some of the heavily damaged cells at the G2 phase that were unable to progress to mitosis. To verify this important issue, calyculin A was used to enable the analysis of unstable and stable aberrations in all the cells progressing through the G2 phase (G2-PCCs), including those heavily damaged cells that were either temporarily or permanently arrested at the G2-phase. As expected, only a modest decline in chromosomal aberrations was observed in G2-PCCs, suggesting that the higher level of aberration reduction seen in the metaphase chromosomes may likely be due to the inability of a subset of heavily damaged cells to progress to the metaphase stage. This notion was substantiated by the increased frequencies (1.3-2.2 folds) of the unstable aberrations in the G2-PCCs relative to metaphase chromosomes. The UHDR irradiation with doses of 6-18 Gy at dose rates of 200-300 Gy/sec was shown to induce apoptotic death and G2 arrest in immortalized human cells.[45] Because hypoxia can reduce the formation of free radicals, a transient depletion of oxygen by UHDR may induce reduced levels of DNA damage, as proposed in the earlier studies.[46,23,47,41] Hypoxia can either enhance or inhibit the activity of various DNA repair pathways (Base Excision Repair, Mismatch Repair and Homologous Recombination Repair) based on the chronic and acute levels of radiation exposures,[48] but the effects of hypoxia were not investigated in this study.

Our study has demonstrated that UHDR results in differentially reduced yields of unstable and stable chromosomal aberrations in both metaphase chromosomes and G2-PCCs, but the underlying mechanisms are not clearly understood. Further studies using well-defined human equivalent model systems are required for evaluating the effects of UHDR radiation on DNA repair and cell cycle regulatory mechanisms. Additionally, some of the inherent confounding factors, such as inter-individual radiation sensitivity/susceptibility, DNA repair efficiency, and gender-specific differences in radio response, need to be evaluated for effectively utilizing the potential of FLASH-RT for successful cancer treatment.

References

1. **Kim MM, Zou W.** Ultra-high dose rate FLASH radiation therapy for cancer. *Med Phys.* 2023;**50** Suppl 1:58–61.
2. **Lin B, Huang D, Gao F,** et al. Mechanisms of FLASH effect. *Front Oncol.* 2022;**12**:995612.
3. **Lv Y, Lv Y, Wang Z,** et al. FLASH radiotherapy: a promising new method for radiotherapy. *Oncol Lett.* 2022;**24**(6):419.
4. **Atkinson J, Bezak E, Le H,** et al. The current status of FLASH particle therapy: a systematic review. *Phys Eng Sci Med.* 2023;**46**(2): 529–560.
5. **Vozenin MC, De Fornel P, Petersson K,** et al. The advantage of FLASH radiotherapy confirmed in mini-pig and cat-cancer patients. *Clin Cancer Res.* 2019;**25**(1):35–42.
6. **Cucinotta FA, Smirnova OA.** Effects of flash radiotherapy on blood lymphocytes in humans and small laboratory animals. *Radiat Res.* 2023; **199**(3):240–251.
7. **Bourhis J, Sozzi WJ, Jorge PG,** et al. Treatment of a first patient with FLASH-radiotherapy. *Radiother Oncol.* 2019;**139**:18–22.
8. **Sammer M, Rousseti A, Girst S,** et al. Longitudinally heterogeneous tumor dose optimizes proton broadbeam, interlaced minibeam, and FLASH therapy. *Cancers (Basel).* 2022;**14**(20):5162.
9. **Shukla S, Saha T, Rama N,** et al. Ultra-high dose-rate proton FLASH improves tumor control. *Radiother Oncol.* 2023;**186**:109741.
10. **Soto LA, Casey KM, Wang J,** et al. FLASH irradiation results in reduced severe skin toxicity compared to conventional-dose-rate irradiation. *Radiat Res.* 2020;**194**(6):618–624.
11. **Fouillade C, Curras-Alonso S, Giuranno L,** et al. FLASH irradiation spares lung progenitor cells and limits the incidence of radio-induced senescence. *Clin Cancer Res.* 2020;**26**(6):1497–1506.
12. **Dewey DL, Boag JW.** Modification of the oxygen effect when bacteria are given large pulses of radiation. *Nature.* 1959;**183**(4673):1450–1451.
13. **Beckers C, Pruschy M, Vetrugno I.** Tumor hypoxia and radiotherapy: a major driver of resistance even for novel radiotherapy modalities. *Semin Cancer Biol.* 2024;**98**:19–30.
14. **Jo HJ, Oh T, Lee YR,** et al. FLASH Radiotherapy: a FLASHing idea to preserve neurocognitive function. *Brain Tumor Res Treat.* 2023;**11**(4):223–231.
15. **Scarmelotto A, Delprat V, Michiels C,** et al. The oxygen puzzle in FLASH radiotherapy: a comprehensive review and experimental outlook. *Clin Transl Radiat Oncol.* 2024;**49**:100860.
16. **Wilson JD, Hammond EM, Higgins GS,** et al. Ultra-high dose rate (FLASH) radiotherapy: silver bullet or fool's gold? *Front Oncol.* 2019;**9**:1563.

17. **Hageman E**, **Che PP**, **Dahele M**, et al. Radiobiological aspects of FLASH radiotherapy. *Biomolecules.* 2022;**12**(10):1376.

18. **Jansen J**, **Knoll J**, **Beyreuther E**, et al. Does FLASH deplete oxygen? Experimental evaluation for photons, protons, and carbon ions. *Med Phys.* 2021;**48**(7):3982–3990.

19. **Hu A**, **Qiu R**, **Li WB**, et al. Radical recombination and antioxidants: a hypothesis on the FLASH effect mechanism. *Int J Radiat Biol.* 2023;**99**(4): 620–628.

20. **Labarbe R**, **Hotoiu L**, **Barbier J**, et al. A physicochemical model of reaction kinetics supports peroxyl radical recombination as the main determinant of the FLASH effect. *Radiother Oncol.* 2020;**153**:303–310.

21. **Geirnaert F**, **Kerkhove L**, **Montay-Gruel P**, et al. Exploring the metabolic impact of FLASH radiotherapy. *Cancers (Basel).* 2025;**17**(1):133.

22. **Wardman P.** Radiotherapy using high-intensity pulsed radiation beams (FLASH): a radiation-chemical perspective. *Radiat Res.* 2020;**194**(6):607–617.

23. **Cooper CR**, **Jones DJL**, **Jones GDD**, et al. Comet assay profiling of FLASH-induced damage: mechanistic insights into the effects of FLASH irradiation. *Int J Mol Sci.* 2023;**24**(8):7195.

24. **Acharya S**, **Bhat NN**, **Joseph P**, et al. Dose rate effect on micronuclei induction in human blood lymphocytes exposed to single pulse and multiple pulses of electrons. *Radiat Environ Biophys.* 2011;**50**(2):253–263.

25. **Kirby-Smith JS**, **Dolphin GW**. Chromosome breakage at high radiation dose-rates. *Nature.* 1958;**182**(4630):270–271.

26. **Prempree T**, **Michelsen A**, **Merz T.** The repair time of chromosome breaks induced by pulsed x-rays on ultra-high dose-rate. *Int J Radiat Biol Relat Stud Phys Chem Med.* 1969;**15**(6):571–574.

27. **Purrott RJ**, **Reeder EJ**. Chromosome aberration yields induced in human lymphocytes by 15 MeV electrons given at a conventional dose-rate and in microsecond pulses. *Int J Radiat Biol Relat Stud Phys Chem Med.* 1977; **31**(3):251–256.

28. **Buonanno M**, **Grilj V**, **Brenner DJ**. Biological effects in normal cells exposed to FLASH dose rate protons. *Radiother Oncol.* 2019;**139**:51–55.

29. **Garty G**, **Obaid R**, **Deoli N**, et al. Ultra-high dose rate FLASH irradiator at the radiological research accelerator facility. *Sci Rep.* 2022;**12**(1):22149.

30. **Cooper CR**, **Jones D**, **Jones GD**, et al. FLASH irradiation induces lower levels of DNA damage ex vivo, an effect modulated by oxygen tension, dose, and dose rate. *Br J Radiol.* 2022;**95**(1133):20211150.

31. **Friedl AA**, **Prise KM**, **Butterworth KT**, et al. Radiobiology of the FLASH effect. *Med Phys.* 2022;**49**(3):1993–2013.

32. **Ahsan A**, **Hiniker SM**, **Davis MA**, et al. Role of cell cycle in epidermal growth factor receptor inhibitor-mediated radiosensitization. *Cancer Res.* 2009;**69**(12):5108–5114.

33. **Swarts SG**, **Flood AB**, **Swartz HM**. Implications of "flash" radiotherapy for biodosimetry. *Radiat Prot Dosimetry.* 2023;**199**(14):1450–1459.

34. **Smith TL**, **Ryan TL**, **Escalona MB**, et al. Application of FISH based G2-PCC assay for the cytogenetic assessment of high radiation dose exposures: Potential implications for rapid triage biodosimetry. *PLoS One.* 2024; **19**(10):e0312564.

35. **Sun M**, **Moquet J**, **Barnard S**, et al. Simplified calyculin A-induced Premature Chromosome Condensation (PCC) protocol for the biodosimetric analysis of high-dose exposure to gamma radiation. *Radiat Res.* 2020; **193**(6):560–568.

36. **Livingston GK**, **Escalona M**, **Foster A**, et al. Persistent in vivo cytogenetic effects of radioiodine therapy: a 21-year follow-up study using multicolor FISH. *J Radiat Res.* 2018;**59**(1):10–17.

37. **Livingston GK**, **Ryan TL**, **Escalona MB**, et al. Retrospective evaluation of cytogenetic effects induced by internal radioiodine exposure: a 27-year follow-up study. *Cytogenet Genome Res.* 2023;**163**(3-4):154–162.

38. **Livingston GK**, **Ryan TL**, **Smith TL**, et al. Detection of simple, complex, and clonal chromosome translocations induced by internal radioiodine exposure: a cytogenetic follow-up case study after 25 years. *Cytogenet Genome Res.* 2019;**159**(4):169–181.

39. **Barghouth PG**, **Melemenidis S**, **Montay-Gruel P**, et al. FLASH-RT does not affect chromosome translocations and junction structures beyond that of CONV-RT dose-rates. *Radiother Oncol.* 2023;**188**:109906.

40. **Barghouth PG**, **Melemenidis S**, **Montay-Gruel P**, et al. FLASH-RT does not affect chromosome translocations and junction structures beyond that of CONV-RT dose-rates. *bioRxiv.* 2023.03.27.534408.

41. **Okoro CM**, **Schüler E**, **Taniguchi CM**. The therapeutic potential of FLASH-RT for pancreatic cancer. *Cancers (Basel).* 2022;**14**(5):1167.

42. **Zhu H**, **Li J**, **Deng X**, et al. Modeling of cellular response after FLASH irradiation: a quantitative analysis based on the radiolytic oxygen depletion hypothesis. *Phys Med Biol.* 2021;**66**:185009.

43. **Sforza D**, **Bunz F**, **Wong J**, et al. Effect of ultrahigh dose rate on biomolecular radiation damage. *Radiat Res.* 2024;**202**(6):825–836.

44. **Löbrich M**, **Jeggo PA**. The impact of a negligent G2/M checkpoint on genomic instability and cancer induction. *Nat Rev Cancer.* 2007;**7**(11):861–869.

45. **Iwata H**, **Toshito T**, **Omachi C**, et al. Proton FLASH irradiation using a synchrotron accelerator: differences by irradiation positions. *Int J Radiat Oncol Biol Phys.* 2025;**121**(5):1293–1302.

46. **Pratx G**, **Kapp DS**. A computational model of radiolytic oxygen depletion during FLASH irradiation and its effect on the oxygen enhancement ratio. *Phys Med Biol.* 2019;**64**(18):185005.

47. **Abolfath R**, **Grosshans D**, **Mohan R**. Oxygen depletion in FLASH ultra-high-dose-rate radiotherapy: a molecular dynamics simulation. *Med Phys.* 2020;**47**(12):6551–6561.

48. **Kaplan AR**, **Glazer PM**. Impact of hypoxia on DNA repair and genome integrity. *Mutagenesis.* 2020;**35**(1):61–68.